Materials for the course

The course is based on book "*Mathematical Modeling and Computation in Finance: With Exercises and Python and MATLAB Computer Codes*", by C.W. Oosterlee and L.A. Grzelak, World Scientific Publishing Europe Ltd, 2019. For more details go here.

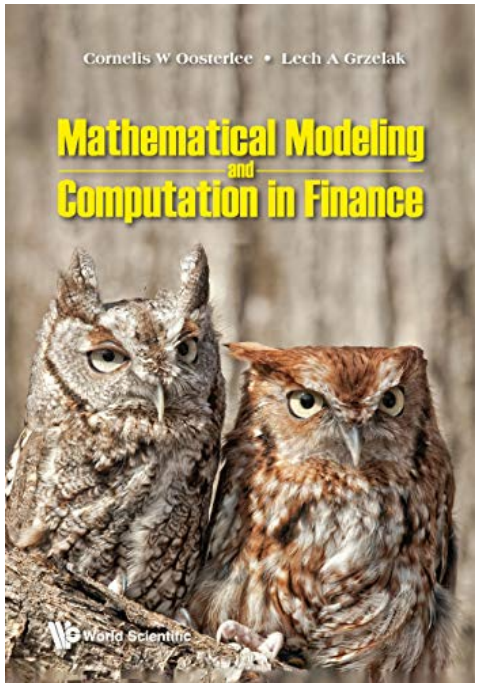

- YouTube Channel with courses can be found here.
- Slides and the codes can be found here.

List of content

Option Pricing with Monte Carlo

- We take $S(t_0) = 5$, $\sigma = 0.3$, $r = 0.06$, $T = 1$, the number of Monte Carlo time steps $m = 1000$ (so that $\Delta t = 1/1000$) and compare the obtained call option values with the analytic solutions from the Black-Scholes formula, for the strike price $K = S(t_0)$, i.e. $V_c(t_0, S(t_0)) = 0.7359$.
- Table below shows that both methods require a similar number of paths to achieve satisfactory pricing results. This is an indication that the Euler and Milstein schemes exhibit the *same order of weak convergence*.

Table: Call option prices in dependence of the number of Monte Carlo paths for the Euler and Milstein discretizations.

Type:	N	100	1000	5000	10000	50000	100000	BS
Europ. call	Euler	0.7709	0.7444	0.7283	0.7498	0.7328	0.7356	0.7359
	Milstein	0.7690	0.7438	0.7283	0.7497	0.7327	0.7356	
Digital call	Euler	2.8253	2.4062	2.4665	2.4411	2.4502	2.4469	2.4483
	Milstein	2.8253	2.4062	2.4674	2.4406	2.4515	2.4462	

Challenges with Standard Discretization Schemes

- A typical example of a process with probability mass around zero is the CIR process, which was discussed to model the variance for the Heston stochastic volatility model with the following dynamics,

$$\boxed{\mathrm{d}v(t) = \kappa(\bar{v} - v(t))\mathrm{d}t + \gamma\sqrt{v(t)}\mathrm{d}W(t), \quad v(t_0) > 0.} \tag{1}$$

- It is well-known that if the Feller condition, $2\kappa\bar{v} > \gamma^2$, is satisfied, the process $v(t)$ cannot reach zero, and if this condition does not hold the origin is accessible and strongly reflecting.
- In both cases, the $v(t)$ process cannot become negative.

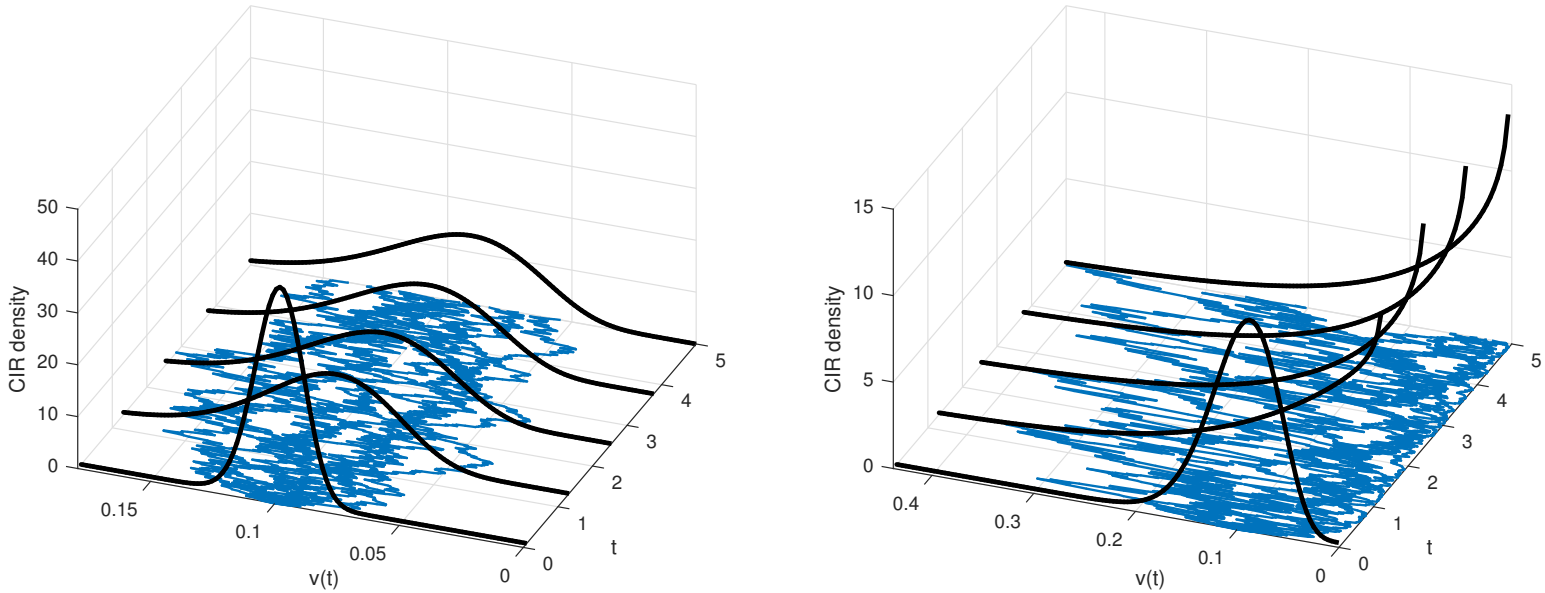

Figure: Paths and the corresponding PDF for the CIR process (1) in the cases where the Feller condition is satisfied and is not satisfied. Simulations were performed with $\kappa = 0.5$, $v_0 = 0.1$, $\bar{v} = 0.1$. Left: $\gamma = 0.1$; Right: $\gamma = 0.35$.

Probability of Negative Realization

- The nonnegativity problem becomes apparent when a standard discretization is employed. If we apply, for example, the Euler discretization to the process in (1), i.e.,

$$v_{i+1} = v_i + \kappa(\bar{v} - v_i)\Delta t + \gamma\sqrt{v_i}\sqrt{\Delta t}Z.$$

and assume that $v_i > 0$, we may calculate the *probability* that a next realization, v_{i+1}, becomes negative, i.e. $\mathbb{P}[v_{i+1} < 0]$.

$$\begin{aligned}\mathbb{P}[v_{i+1} < 0 | v_i > 0] &= \mathbb{P}[v_i + \kappa(\bar{v} - v_i)\Delta t + \gamma\sqrt{v_i \Delta t}Z < 0 | v_i > 0] \\ &= \mathbb{P}[\gamma\sqrt{v_i \Delta t}Z < -v_i - \kappa(\bar{v} - v_i)\Delta t | v_i > 0],\end{aligned}$$

which equals,

$$\mathbb{P}[v_{i+1} < 0 | v_i > 0] = \mathbb{P}\left[Z < -\frac{v_i + \kappa(\bar{v} - v_i)\Delta t}{\gamma\sqrt{v_i \Delta t}} \middle| v_i > 0\right] > 0.$$

- Since Z is a normally distributed random variable, it is unbounded. Therefore the probability of v_i becoming negative, is positive under the Euler discretization, implying $\mathbb{P}[v_{i+1} < 0 | v_i > 0] > 0$.

Truncated Euler Scheme

- The truncated Euler scheme, as the name says, is based on the previously introduced Euler discretization scheme. In order to prevent the process to cross the axis, we need to deal with possible negative path realizations v_{i+1}.
- It can be summarized, as follows,

$$\begin{cases} \hat{v}_{i+1} = v_i + \kappa(\bar{v} - v_i)\Delta t + \gamma\sqrt{v_i \Delta t}Z, \\ v_{i+1} = \max(\hat{v}_{i+1}, 0). \end{cases}$$

- Although the scheme certainly provides paths that are nonnegative, the accuracy of this scheme is parameter-dependent, meaning that, when the Feller condition is not satisfied and the density should accumulate around zero, the *adjusted paths*, due to the truncation, may be highly biased. In essence, by the truncation a different process than the original CIR process is represented numerically.
- When truncation takes place for many Monte Carlo paths, the accuracy may be limited as the discretization bias could be high.

Reflecting Euler Scheme

- One of the important properties of the CIR process is that the origin is attainable, however, it is *not* an absorbing boundary. This means that the Monte Carlo paths may *reach* the boundary $v = 0$, but they cannot stay at the boundary – they should immediately move away from it. When using the truncated Euler scheme from above, using $v_{i+1} = \max(\hat{v}_{i+1}, 0)$, the paths that attain negative values are projected at the origin.
- Another possible modification for the simulation of the CIR process, which is particularly useful when the Feller condition is not satisfied, is to use the so-called *reflecting principle*, where the variance paths are forced to move upwards again.
- The reflecting scheme is given by the following adjustment of the Euler scheme,

$$\begin{cases} \hat{v}_{i+1} = v_i + \kappa(\bar{v} - v_i)\Delta t + \gamma\sqrt{v_i \Delta t} Z, \\ v_{i+1} = \left|\hat{v}_{i+1}\right|. \end{cases} \tag{2}$$

Comparison of the Reflecting and Truncated Euler Schemes

- In Figure below, some paths that were generated by the reflecting and truncated Euler schemes are compared. The paths that are generated by both schemes are essentially the same, until they reach the boundary at $v(t) = 0$. After hitting the origin, the reflecting scheme will have paths that are above those that are generated by the truncation scheme. Notice that by the reflecting scheme we however *do not improve* the quality of the Euler scheme.

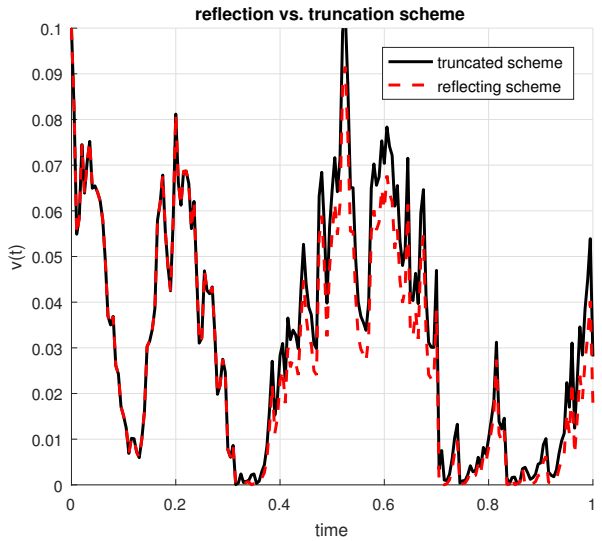

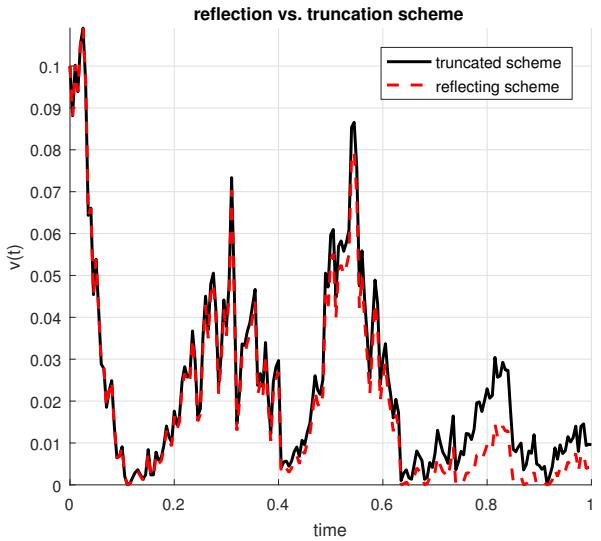

- Let us take a look at Python code.

Exact Simulation of the CIR Model

- A different approach for simulating paths from the CIR process takes into account the fact that variance process $v(t)$, follows the *noncentral chi-squared distribution*. Details of the noncentral chi-squared distribution have been given already in previous lecture in the context of the Heston stochastic volatility model.
- Conditional on state $v(s)$, $s < t$, the distribution at time t is given by,

$$\boxed{v(t)|v(s) \sim \bar{c}(t,s) \cdot \chi^2(\delta, \bar{\kappa}(t,s)),} \tag{3}$$

with

$$\bar{c}(t,s) = \frac{\gamma^2}{4\kappa}\left(1 - \mathrm{e}^{-\kappa(t-s)}\right), \quad \delta = \frac{4\kappa\bar{v}}{\gamma^2}, \quad \bar{\kappa}(t,s) = \frac{4\kappa \mathrm{e}^{-\kappa(t-s)}}{\gamma^2\left(1 - \mathrm{e}^{-\kappa(t-s)}\right)} v(s).$$

Exact Simulation of the CIR Model

- Given formulation may form the basis for an *exact simulation scheme* for the path realizations of the CIR process, as, for $i = 0, \ldots, m-1$,

$$\begin{aligned} \bar{c}(t_{i+1}, t_i) &= \frac{\gamma^2}{4\kappa}\left(1 - \mathrm{e}^{-\kappa(t_{i+1}-t_i)}\right), \\ \bar{\kappa}(t_{i+1}, t_i) &= \frac{4\kappa \mathrm{e}^{-\kappa(t_{i+1}-t_i)}}{\gamma^2\left(1 - \mathrm{e}^{-\kappa(t_{i+1}-t_i)}\right)} \boxed{v_i}. \\ \boxed{v_{i+1}} &= \bar{c}(t_{i+1}, t_i)\chi^2(\delta, \bar{\kappa}(t_{i+1}, t_i)), \end{aligned}$$

  with a constant parameter $\delta = 4\kappa\bar{v}/\gamma^2$, and some initial value $v(t_0) = v_0$.
- Let us revisit Python code.

The Heston Model

- The Heston model is governed by the following dynamics:

$$\begin{cases} \mathrm{d}S(t) = rS(t)\mathrm{d}t + S(t)\sqrt{v(t)}\mathrm{d}W_x(t), \\ \mathrm{d}v(t) = \kappa(\bar{v} - v(t))\mathrm{d}t + \gamma\sqrt{v(t)}\mathrm{d}W_v(t), \end{cases} \tag{4}$$

- Which for $X(t) := \log S(t)$, becomes:

$$\begin{cases} \mathrm{d}X(t) = \left(r - \frac{1}{2}v(t)\right)\mathrm{d}t + \sqrt{v(t)}\mathrm{d}W_x(t), \\ \mathrm{d}v(t) = \kappa(\bar{v} - v(t))\mathrm{d}t + \gamma\sqrt{v(t)}\mathrm{d}W_v(t), \end{cases} \tag{5}$$

  with correlation $\mathrm{d}W_x(t)\mathrm{d}W_v(t) = \rho_{x,v}\mathrm{d}t$,

- which in terms in independent Brownian motions is given by:

$$\begin{cases} \mathrm{d}X(t) = \left(r - \frac{1}{2}v(t)\right)\mathrm{d}t + \sqrt{v(t)}\left[\rho_{x,v}\mathrm{d}\widetilde{W}_v(t) + \sqrt{1-\rho_{x,v}^2}\mathrm{d}\widetilde{W}_x(t)\right], \\ \mathrm{d}v(t) = \kappa\left(\bar{v} - v(t)\right)\mathrm{d}t + \gamma\sqrt{v(t)}\mathrm{d}\widetilde{W}_v(t). \end{cases}$$

Almost Exact Discretization of the Heston Model

- After integration of both processes in a certain time interval $[t_i, t_{i+1}]$, the following discretization scheme is obtained:

$$\begin{aligned} x_{i+1} &= x_i + \int_{t_i}^{t_{i+1}} \left(r - \frac{1}{2} v(t) \right) \mathrm{d}t + \rho_{x,v} \boxed{\int_{t_i}^{t_{i+1}} \sqrt{v(t)} \mathrm{d}\widetilde{W}_v(t)} \\ &+ \sqrt{1-\rho_{x,v}^2} \int_{t_i}^{t_{i+1}} \sqrt{v(t)} \mathrm{d}\widetilde{W}_x(t), \end{aligned}$$

and

$$v_{i+1} = v_i + \kappa \int_{t_i}^{t_{i+1}} (\bar{v} - v(t)) \, \mathrm{d}t + \gamma \boxed{\int_{t_i}^{t_{i+1}} \sqrt{v(t)} \mathrm{d}\widetilde{W}_v(t)}.$$

- Notice that the two integrals with $\widetilde{W}_v(t)$ in the SDEs above are the same, and in terms of the variance realizations they are given by:

$$\boxed{\int_{t_i}^{t_{i+1}} \sqrt{v(t)} \mathrm{d}\widetilde{W}_v(t)} = \frac{1}{\gamma} \left(v_{i+1} - v_i - \kappa \int_{t_i}^{t_{i+1}} (\bar{v} - v(t)) \mathrm{d}t \right). \tag{7}$$

Almost Exact Discretization of the Heston Model

- The variance v_{i+1} can then be simulated, for given value of v_i, by means of the CIR process, or, equivalently, by either the noncentral chi-squared distribution or by the QE scheme (the techniques described in the book).
- As a final step in the Heston model simulation, the discretization for x_{i+1} is given by:

$$\begin{aligned} x_{i+1} &= x_i + \int_{t_i}^{t_{i+1}} \left(r - \frac{1}{2} v(t) \right) \mathrm{d}t \\ &+ \frac{\rho_{x,v}}{\gamma} \left(v_{i+1} - v_i - \kappa \int_{t_i}^{t_{i+1}} (\bar{v} - v(t)) \, \mathrm{d}t \right) \\ &+ \sqrt{1 - \rho_{x,v}^2} \int_{t_i}^{t_{i+1}} \sqrt{v(t)} \mathrm{d}\widetilde{W}_x(t). \end{aligned}$$

Almost Exact Discretization of the Heston Model

- We approximate all integrals appearing in the expression above by their left integration boundary values of the integrand, as in the Euler discretization scheme:

$$\begin{aligned} x_{i+1} &\approx x_i + \int_{t_i}^{t_{i+1}} \left(r - \frac{1}{2} v_i \right) \mathrm{d}t \\ &+ \frac{\rho_{x,v}}{\gamma} \left(v_{i+1} - v_i - \kappa \int_{t_i}^{t_{i+1}} (\bar{v} - v_i) \, \mathrm{d}t \right) \\ &+ \sqrt{1 - \rho_{x,v}^2} \int_{t_i}^{t_{i+1}} \sqrt{v_i} \mathrm{d}\widetilde{W}_x(t). \end{aligned}$$

- The calculation of the integrals is now trivial and results in:

$$\begin{aligned} x_{i+1} &\approx x_i + \left(r - \frac{1}{2} v_i \right) \Delta t + \frac{\rho_{x,v}}{\gamma} \left(v_{i+1} - v_i - \kappa \left(\bar{v} - v_i \right) \Delta t \right) \\ &+ \sqrt{1 - \rho_{x,v}^2} \sqrt{v_i} \left(\widetilde{W}_x(t_{i+1}) - \widetilde{W}_x(t_i) \right). \end{aligned} \tag{8}$$

Almost Exact Discretization of the Heston Model

- Finally for $\widetilde{W}_x(t_{i+1}) - \widetilde{W}_x(t_i) \stackrel{\mathrm{d}}{=} \sqrt{\Delta t} Z_x$, with $Z_x \sim \mathcal{N}(0,1)$, we find:

$$\begin{cases} x_{i+1} \approx x_i + k_0 + k_1 v_i + k_2 v_{i+1} + \sqrt{k_3 v_i} Z_x, \\ v_{i+1} = \bar{c}(t_{i+1}, t_i) \chi^2(\delta, \bar{\kappa}(t_{i+1}, t_i)), \end{cases}$$

- with the variance process simulated as follows:

$$\begin{aligned} \bar{c}(t_{i+1}, t_i) &= \frac{\gamma^2}{4\kappa}(1 - \mathrm{e}^{-\kappa(t_{i+1} - t_i)}), \quad \delta = \frac{4\kappa\bar{v}}{\gamma^2}, \\ \bar{\kappa}(t_{i+1}, t_i) &= \frac{4\kappa \mathrm{e}^{-\kappa \Delta t}}{\gamma^2(1 - \mathrm{e}^{-\kappa \Delta t})} v_i, \end{aligned}$$

and $\chi^2(\delta, \bar{\kappa}(\cdot,\cdot))$ the noncentral chi-squared distribution with δ degrees of freedom and noncentrality parameter $\bar{\kappa}(t_{i+1}, t_i)$ and

$$\begin{aligned} k_0 &= \left(r - \frac{\rho_{x,v}}{\gamma}\kappa\bar{v}\right)\Delta t, \quad k_1 = \left(\frac{\rho_{x,v}\kappa}{\gamma} - \frac{1}{2}\right)\Delta t - \frac{\rho_{x,v}}{\gamma}, \\ k_2 &= \frac{\rho_{x,v}}{\gamma}, \quad k_3 = (1 - \rho_{x,v}^2)\Delta t. \end{aligned}$$

European Option Pricing with Almost Exact Simulation

- In this simulation experiment, European call options are computed by means of the AES scheme, with $S(t_0) = 100$, for three different strike prices: $K = 100$ (ATM), $K = 70$ (ITM) and $K = 140$ (OTM). In the experiment different time steps are used, varying from one time step per year to 64 time steps per year.
- The model parameters are chosen as:

$$\kappa = 0.5, \gamma = 1, \bar{v} = 0.04, v_0 = 0.04, r = 0.1, \rho_{x,v} = -0.9.$$

- The numerical results are based on 500.000 Monte Carlo paths, They are presented in Table 17. The reference results have been generated by the COS method.

	$K = 100$		$K = 70$		$K = 140$	
Δt	Euler	AES	Euler	AES	Euler	AES
1	0.94 (0.023)	-1.00 (0.012)	-0.82 (0.028)	-0.53 (0.016)	1.29 (0.008)	0.008 (0.001)
1/2	2.49 (0.022)	-0.45 (0.011)	-0.11 (0.030)	-0.25 (0.016)	1.03 (0.008)	-0.0006 (0.001)
1/4	2.40 (0.016)	-0.18 (0.010)	0.37 (0.027)	-0.11 (0.016)	0.53 (0.005)	0.0005 (0.001)
1/8	2.08 (0.016)	-0.10 (0.010)	0.43 (0.025)	-0.07 (0.016)	0.22 (0.003)	0.0009 (0.001)
1/16	1.77 (0.015)	-0.03 (0.010)	0.40 (0.023)	-0.03 (0.016)	0.08 (0.001)	0.0002 (0.001)
1/32	1.50 (0.014)	-0.03 (0.009)	0.34 (0.022)	-0.01 (0.016)	0.03 (0.001)	-0.002 (0.001)
1/64	1.26 (0.013)	-0.001 (0.009)	0.27 (0.021)	-0.005 (0.016)	0.02 (0.001)	0.001 (0.001)